Preparation of PFCs for the Efficient use in ITER and DEMO Plasma-Wall Interaction Studies within the EUROfusion Consortium

S. Brezinsek[1], J.W. Coenen[1], T. Schwarz-Selinger[2], K. Schmid[2], A. Kirschner[1], A. Hakola[3], F.L. Tabares[4], H. van der Meiden[5], M.-L. Mayoral[6], M. Reinhart[1], E. Tsitrone[7] and WP PFC contributors (see http://www.euro-fusionscipub.org/PFC)[*]

[1]Forschungszentrum Jülich GmbH, Institut für Energie- und Klimaforschung Plasmaphysik, Partner of the Trilateral Euregio Cluster (TEC), 52425 Jülich, Germany
[2]Max-Planck-Institut für Plasmaphysi, D-85748 Garching, Germany
[3]VTT Technical Research Centre of Finland Ltd., P. O. Box 1000, 02044 VTT, Finland
[4]CIEMAT, Av Complutense 40, 28040 Madrid, Spain
[5]FOM Institute DIFFER, Eindhoven, the Netherlands
[6]CCFE Fusion Association, Culham Science Centre, Abingdon, OX143DB, UK
[7]CEA, IRFM, F-13108 Saint Paul Lez Durance, France
Corresponding Author: s.brezinsek@fz-juelich.de

1 Introduction

Particle and power exhaust is a key area of current fusion research and mandatory for a successful operation of ITER and DEMO - the first reactor-like device. The importance of this area as well as the need to provide a solution for the plasma-facing interface has been identified in Europe in the so-called fusion roadmap [1] resulting in a dedicated programm covering tokamak as well as laboratory research studies in linear plasma devices, electron-beam, neutral-beam, and ion-beam loading facilities. The interconnection of both research areas is done via common experimental physics studies, specification and qualification of plasma-facing components (PFCs) in the different loading facilities, and, most importantly, by simulation of plasma exhaust and plasma-material interaction [2] starting from basic process modeling by e.g. molecular dynamics (MD [3]) to integrated tokamak modelling by e.g. global erosion-deposition codes (ERO [4], WALLDYN [5] etc.) and plasma boundary codes (SOLPS [2], SOLEDGE-EIRENE [6] etc.). Thereby, the plasma and particle exhaust solution must ensure the compatibility of the PFC power handling with plasma edge conditions required for good plasma confinement during quasi steady-state operation for hundreds of plasma seconds as foreseen in ITER and beyond [7]. Laboratory heat load facilities (JUDITH [8], GLADIS [9] etc.) and linear plasmas (PSI-2 [10], Pilot-PSI [11], MAGNUM etc.) are presently essential to predict the PFC performance at high particle fluence $\phi > 10^{27}D^+m^{-2}$) and number of thermal cycles ($> 10^6$ ELM-like events) as expected in such quasi-state conditions. Current experiments in JET [12] and ASDEX Upgrade [13] are used to verify solutions for tens of plasma seconds without active cooling of PFCs, but long-pulse steady-state operation in the complex tokamak environment will be available in the near future in WEST [14] for complementary studies to the corresponding laboratory experiments.

The EUROfusion work package plasma-facing components, the successor of the EFDA task force for plasma-wall interaction [15], is addressing these critical points in order to ensure the reliable and efficient use of conventional (solid metallic) plasma-facing components in ITER (made of tungsten and beryllium [16]) and DEMO (made of tungsten and reduced-activation ferritic martensitic (RAFM) steel [17]) with respect to heat load capabilities (transient and steady-state heat and particle loads), lifetime estimates (erosion, material mixing, and surface morphology), and safety aspects (fuel retention, fuel removal, material migration, and dust formation). Thereby, the development of plasma edge and plasma-surface interaction diagnostics used to determine physics quantities such as electron density, electron temperature, ion energy or impinging ion flux and composition is performed in a dedicated supporting activity providing crucial input in particular to the modelling activities. Successfully qualified diagnostics or concepts such as e.g. Laser-Induced Breakdown Spectroscopy (LIBS), optimised to determine the fuel content (mixed hydrogenic fuel and helium) and material composition in metallic plasma-facing materials exposed to divertor-like plasma conditions [18], will be transferred to the tokamak environment. These different activities are coordinated within six sub projects all aiming to support the conventional PFC solution with solid metallic components and i.e. a full tungsten divertor following the step ladder approach (AUG to JET to ITER to DEMO). In addition also one sub project is following the back-up solution via liquid metals [19] as alternative PFC concepts to deal with the high power loads at high wall temperatures in DEMO ensuring the required low fuel retention to close the fuel cycle in the reactor. We present in the following subsections a few key results of the coordinated studies within WP PFC addressing ITER and DEMO related issues.

2 Synergistic effects in heat and particle loading of W

One of the most critical question of transient heat load experiments on ITER-relevant materials like tungsten is whether the obtained limits can be extrapolated to power and heat flux conditions expected during ELM excursions in the divertor. Most available techniques can match single parameters (e.g. the heat flux factor), but full experimental matching of the power and particle flux densities, the impact energy spectrum, the plasma conditions and impurity composition expected in ITER cannot be achieved. A series of expositions with combined particle and heat load on reference W plasma-facing material were carried out to identify synergistic effects with respect to material properties such as hardness, ductility, and microstructure as well as erosion, retention, and mixing by load execution in sequence or simultaneously. In combination with loading parameters such as the surface temperature a detailed mapping of the impact of synergy effects accompanied e.g. with helium or hydrogen exposure could be documented [20] leading to a complex modification of material properties featuring reduced cracking behaviour in the combined plasma and heat flux exposure by LASER beam in comparison with conventional thermal shock tests in electron beam facilities. Fig. 1 provides the change of W surface morphology by applying (i) first 1000 LASER pulses with a power density of $0.76 GW m^{-2}$ at a max. temperature of $T = 1120K$ followed by PSI-2 plasma exposure in helium (He ion impact energy: $E_{in} = 80 eV$, flux: $\Gamma = 2.8 \times He^{+} 10^{22} m^{-2} s^{-1}$, and fluence: $\phi = 5.6 \times He^{+} 10^{25} m^{-2}$), (ii) simultaneous exposure under similar heat pulse and plasma conditions, and (iii) reversed order with initial plasma exposure followed by ELM-like heat pulses by LASER exposition. The order of exposure determines the final state of surface

modification with W nanostructure formation on the cracked W sample in condition (i), a complex surface structure with remains of the W nanostructure and He nanobubbles in (ii), and surface roughness, near-surface melting and He nanobubbles in (iii). Further
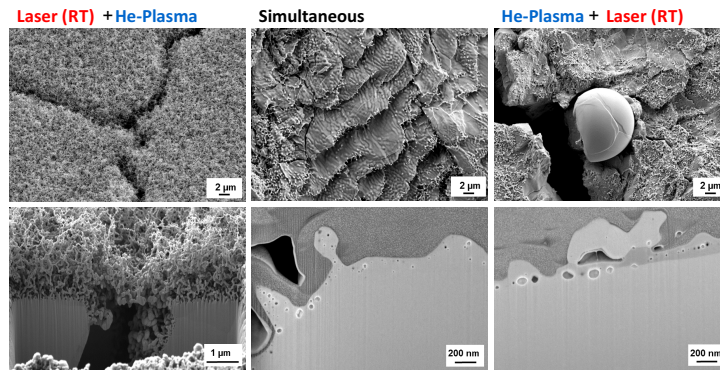

FIG. 1: *Scanning Electron Microscope images and Focused Ion Beam cuts of He-plasma and laser exposed surfaces: (a) and (d) First laser at room temperature than He plasma exposure at $1120K$; (b) and (e) simultaneous laser and He-plasma exposure at $1120K$; (c) and (f) First He plasma at $1120K$ than laser exposure at room temperature [20].*

details of the experiment and its analysis are described in [20]. Corresponding experiments in H plasmas as well as the comparison of heat pulses by e-beam, neutral beam, LASER, and high energy plasma bursts simulating all ELM-like conditions is provided in [21].

These experimental results are leading to a better physics understanding of the impact mechanisms during PFC exposure and are used to develop model descriptions. The latter are then used for predictions of PFC capabilities and operational space, but exposures under tokamak conditions are still desirable to verify the obtained models for ITER and DEMO. Indeed WEST experiments with the associated installations of diagnostics are prepared to bridge laboratory and tokamak experiments and to increase the predictability of PFC performance with minimization of operational risks for ITER.

3 Material migration and W prompt re-deposition

The understanding of material migration, thus the process cycle of material erosion, transport, and deposition is one of the key issues for a successful and safe operation of ITER. The process cycle is associated with the lifetime of first wall material components, predominantly by erosion, and with the safety aspect due to long-term tritium retention and dust formation and release [22]. The latter is in JET as well as in ITER dominated by co-deposition of tritium with Be [23] whereas implantation in W will determine the retention in a full metallic DEMO. The description of the cycle and initial predictions to the material migration and retention pattern in ITER assuming H-mode plasmas in D was successfully done by the WallDYN [5] and ERO [4] codes within WP PFC.

Concerning the life time estimation of W PFCs, emphasis in the ERO modelling was put on description of prompt re-deposition of W, thus the return of eroded and ionized W within one Larmour radius [24]. The inclusion of an improved sheath description obtained from PIC calculations [25] in ERO was used to perform parameter studies covering the typical operational space of the JET tokamak in order to provide the prompt re-deposition fraction of W. ERO modelling of the prompt deposition of sputtered tungsten atoms has

been done for an electron temperature (T_e) range of $1eV$ to $20eV$ and electron density (n_e) range from $1 \times 10^{18} m^{-3}$ to $1 \times 10^{21} m^{-3}$. A magnetic field of $3T$ with a shallow field angle of $2°$ relative to the surface has been used. The resulting fractions of prompt deposition are summarised in fig. 2. For typical JET inter-ELM plasmas ($T_e = 10eV$, 1×10^{19} to 1×10^{20}) the fraction of prompt deposition is between 60% and 90%, which is in fair agreement with experimental observations. During ELM conditions with n_e of 1×10^{20} and T_e of $20eV$ the modelled amount of prompt deposition is about 95%. For
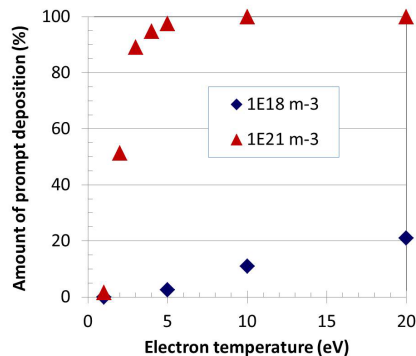

FIG. 2: *Modelled amounts of prompt deposition in dependence on the electron temperature for two different electron densities ($1 \times 10^{18} m^{-3}$ and $1 \times 10^{21} m^{-3}$) [24].*

this simulation the Free Streaming Model [26] has been applied assuming a deuterium ion energy of $1keV$. The self-sputtering yield of returning tungsten ions has been calculated and it seen that for the parameter range studied the yield is always well below one wherefore runaway sputtering does not occur.

The next step in global migration predictions will expand from pure D plasmas in a pure Be/W environment towards a plasma with realistic impurity mixture and include the new laboratory findings on synergistic effects of Ne, N (seeding gas) and He (ash), on erosion, fuel retention and material mixing such as Be_3N_2 [27] or WN production [28], identified to act as diffusion barrier, and formation of co-deposits with Be/D/N. Moreover, dedicated studies on ammonia formation to better understand its production in the plasma and the metallic first wall [29, 30, 31, 32], to assess its potential risk and develop possible mitigation procedures in case nitrogen needs to be used as seeding gas for divertor cooling in the future are also covered. Fundamental studies related to outgassing and the isotope exchange in W, Be and mixed Be-W co-deposits are performed in conjunction with a PISCES-B collaboration [33]. Mixed Be layers have been developed [34] to mimic JET co-deposits and allow the successful qualification of in-situ fuel retention diagnostics such as LIBS and fuel removal techniques such as baking. Reference analysis of the fuel content in plasma-facing materials with post-mortem techniques such as TDS and NRA [35] are used to provide standard values for experiments and modelling as well as to benchmark the quantification with laser-based diagnostics such as LIBS [36, 37, 38] and LIDS.

4 Fuel retention studies in self-damaged W

Till recently all hydrogen retention studies were performed by sequential high energy ion damaging and subsequent plasma/gas/atom loading of the material by hydrogen isotopes. Detailed studies were performed in WP PFC to determine experimentally the retention mechanisms, the isotope exchange, the surface release mechanisms as well as to develop

corresponding complex models for these processes in bare plasma-facing materials as well as co-deposits [39, 40]. However, in a real fusion reactor environment both implantation of energetic hydrogen ions and neutrals as well as damage creation by neutron irradiation will take place at the same time. The consequences of synergistic effects for hydrogen retention in tungsten are unknown but theory predicts defect stabilization in the presence of hydrogen atoms in tungsten [41]. To make one step further towards more realistic situation we
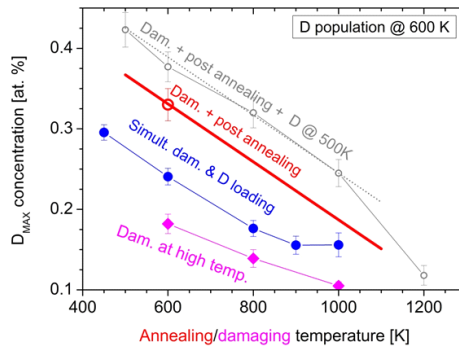

FIG. 3: *Maximum D concentration obtained at the position of the maximum of the peak displacement damage profile versus damaging temperatures obtained from D depth profiles for the damaging at high temperatures (process i)) and simultaneous self-damaging and D loading. The data are compared to damaging at room temperature and afterward post-damaging annealing and defect population by D: damaging process ii) (grey data) and extrapolation for population of defects at 600 K (red data). [42].*

have performed the first experimental study on simultaneous defect creation by $10.8 MeV$ W self-ion implantation and D-atom-beam loading ($E = 0.28eV$, $\Gamma = 5.4 \times 10^{18} Dm^{-2}s^{-1}$) in W between $450K$ and $1000K$. After the damaging and loading D depth profiles were measured by Nuclear Reaction Analysis (NRA) using the $D(^3He, p)^4He$ reaction. In order to determine how many traps were actually created in the material the samples were after simultaneous damaging and loading and NRA analysis exposed to D atoms for additional 19h at $600K$, $\phi = 3.7 \times 10^{23} Dm^{-2}$. As expected the highest concentration was obtained for the $450K$ case, decreasing with damaging temperature. In order to sort out the observed effects comparison to a series of sequential damaging/annealing/exposure experiments is made [42] as depicted in fig. 3. Namely, three sequential experimental series were performed in addition with different damaging/exposure procedures, that help to separate the processes: i) W-ion damaging at elevated temperatures + D-atom exposure at $600K$ afterwards to determine the trap concentration; ii) W-ion damaging at room temperature + samples post-damaging annealing at different temperatures for one hour + D-atom loading at $500K$ afterwards to determine the trap concentration; and iii) W-ion damaging at room temperature + D-atom exposure at elevated temperatures afterwards. Comparison of the maximum deuterium concentration obtained at the maximum of the peak displacement damage for simultaneous self-damaging and D-atom loading and processes under i) and ii) are shown in fig. 3. Synergistic effects were observed, namely, higher D concentrations were found in the case of simultaneous damaging and D-atom loading as compared to sequential damaging at elevated temperatures and populating the defects afterwards. However, the deuterium retention is still lower as compared to sequential damaging at room temperature and post-damaging annealing. The observations

are explained by stabilization of the created defects by the presence of solute hydrogen in the simultaneous case in the bulk that would annihilate at high temperatures without the presence of hydrogen.

5   Preferential sputtering of Fe-W and EUROFER

An example for pure DEMO research within WP PFC are erosion studies on RAFM steels, such as EUROFER, which are foreseen as primary structural material. In certain areas of the main chamber wall in DEMO such as on blanket modules tungsten was foreseen as thin protection coatings on the structural steel to minimize wall erosion which would be otherwise to high due to Fe in the steel leading potentially to high-Z accumulation in the plasma. Recently, EUROFER was proposed directly as plasma-facing material in recessed areas as it provides lower fuel retention and less weight, which would simplify the design and hence reduce cost as well as reduce the risk of coating failure. The reason for RAFM to be applicable is amongst other elements it contains small amounts of W ($0.45at\%$) whose sputtering behaviour will be smaller compared to those of the lighter elements. W is therefore expected to enrich at the surface during the course of operation which would lead to a reduction of the sputter yield with exposition time. To understand the effect quantitatively a model system of W containing Fe layers was developed and exposed in addition to EUROFER to different D ion beams and plasmas to study the erosion in the impact energy range between $100eV$ and $1keV$, target temperatures between room temperature and $770K$ for D fluxes between $10^{17}D^+m^{-2}s^{-1}$ and $10^{21}D^+m^{-2}s^{-1}$ collecting up to a fluence of $6 \times 10^{25}D^+m^{-2}$. To measure erosion and W surface enrichment mass loss, Rutherford Backscattering Spectrometry (RBS), Heavy Ion Elastic Recoil Detection (HIERDA), as well as Secondary Ion Mass Spectrometry (SIMS) was applied. All experiments confirmed the anticipated effect and have proven the W enrichment at the surface at room temperature. Enrichment is maximum when the impact energy is below the sputter threshold for physical sputtering of W ($200eV$ for D^+, $140eV$ for T^+) but is observed also above. At room temperature and for an energy of $200eV/D$ at fluences of $10^2D^+m^{-2}$ enrichment is already observed and saturates at $3 \times 10^{24}D^+m^-2$. Fig.4a shows the sputter yields as function of D fluence for different energies of Fe-W model-system films with different initial W concentrations [43]. However, a quantitative
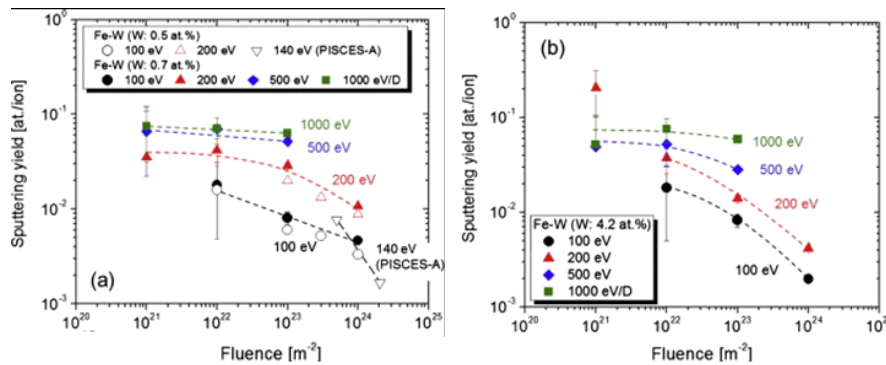

FIG. 4: Fluence dependence of sputtering yields of FeW layers with (a) low W concentrations (0.5 and 0.7at.%) and (b) high W concentration (W concentration: 4.2at.%) [43].

comparison between modelling and experiment is hampered by the limited depth resolu-

tion. Presently Medium Energy and Low Ion Scattering (MEIS and LEIS) is applied to improve this [44]. A recently developed code that combines the simulation of the ionsolid interaction with solid state diffusion predicts that diffusion will set in above $800K$ and will counteract enrichment [?]. However, it is doubtful if is justified to applying the tracer diffusion coefficient for tungsten in Fe for a multi component material such as RAFM steel. Therefore reliable experiments at higher temperatures need to be conducted in the future and in addition a task was started to measure the diffusion coefficient as a function of W concentration. First experiments show that $800K$ might be indeed the critical operation temperature for RAFM steels as PFM material which is just at the nominal wall temperature of DEMO.

6   Liquid metals as alternative PFCs for DEMO

Qualification studies with respect to power loads, erosion rates and fuel retention/removal rates of liquid plasma-facing material solutions made of Sn, Li or Sn/Li alloys are carried out in close relation with design studies dedicated to a new European divertor test tokamak, an intermediate step to DEMO, equipped with a non-conventional divertor [19]. Dedicated plasma compatibility studies with Capillary Porous Systems (CPS) made of LiSn alloys were performed in TJ-II in order to study the fuel retention, hydrogen recycling, and plasma compatibility. Indeed low fuel retention of below $0.01\% = \frac{H}{Sn+Li}$ at $T < 720K$ was measured by TDS. No substantial impact on the plasma operation was observed with intact CPS whereas plasma operation was hampered if the stainless steel structure with liquid metal was exposed [47, 46].   Another important question for liquid
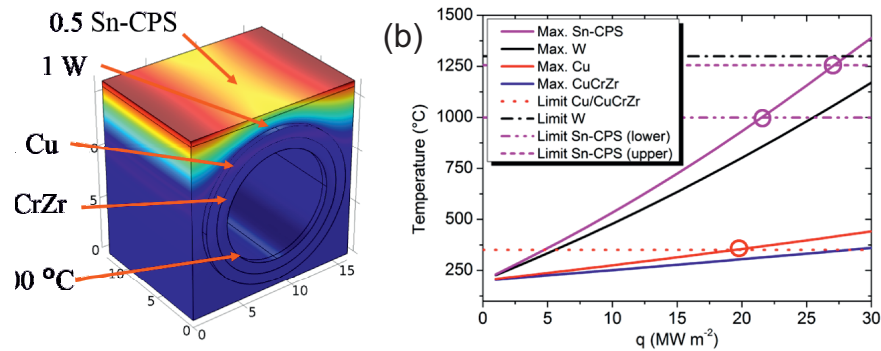

FIG. 5: (a) COMSOL model of a Sn CPS and W based mono block design for DEMO. The inner wall temperature of the water pipe is also shown. (b) The maximum equilibrium temperature for each part of the component and their material temperature limits. The intersection of the limits is shown with a circle [48, 49].

metals is if the power handling capability can be the same or greater than tungsten-based PFCs. To investigate this a Sn-filled CPS target was exposed to a set of He plasma discharges in Pilot-PSI [11] in the range $q = 1.8 - 18MWm^{-2}$ and its performance examined. Following the set of discharges it was observed that there was no damage to the underlying W mesh and that the sample remained wetted by the Sn [48]. No macroscopic erosion, i.e. droplet production, was produced due to the small pore size which provided sufficient capillary restraint. Extrapolation of the performance of such a Sn-filled CPS system by modifying mono block designs towards DEMO using COMSOL finite element modelling

was done [49] indicating the potential of this PFC solution. Indeed heat loads in the range $15 - 20 MWm^{-2}$ could be sustained, dependent on the design, without exceeding the temperature limits for Sn evaporation and those of other materials in the component (fig. 5). Further studies are required to qualify the concept for the DEMO divertor.

7 Summary

WP PFC is addressing the most urgent questions in the area of plasma-wall interaction in depth and complements studies at the major European tokamaks with metallic PFCs. Gained physics understanding and verified modelling ensures rising confidence in the operation with Be/W in ITER and W-based PFCs in DEMO. Further studies are focused on the plasma-wall interaction in the complex regime with multiple impurities, with neutron damage, and with advanced plasma-facing materials.

References

[1] F. Romanelli et al., A roadmap to the realisation of fusion energy ISBN 978-3-00-040720-8
[2] S. Wiesen et al., submitted to Nucl. Mater. Energy (2016) - presented at PSI conference Rom
[3] K. Nordlund et al., J. Phys. D: Appl. Phys. 47 (2014) 224018
[4] A. Kirschner et al., J. Nucl. Mater. **463** (2015) S116
[5] K. Schmid et al., J. Nucl. Mater. **463** (2015) S66
[6] G. Ciarolo et al., submitted to Nucl. Mater. Energy (2016) - presented at PSI conference Rom
[7] M. Wischmeier et al., J. Nucl. Mater. **463** (2015)
[8] P. Majerus et al., Fusion Eng. Des. **7579** (2005) 365369
[9] H. Greuner et al., J. of Nucl. Mater. **367370** (2007) 1444
[10] A. Kreter et al., Fusion Sci. Technol. **68** (2015) 8
[11] G. J. van Rooij et al., Appl. Phys. Lett. **90** (2007) 121501
[12] S. Brezinsek et al., J. Nucl. Mater. **463** (2015) 11
[13] A. Kallenbach et al., Plasma Phys. Control. Fusion **55** (2013) 12404
[14] J. Bucalossi et al., Fusion Eng. Des. **89** (2014) 907
[15] V. Philipps et al., Plasma Phys. Control. Fusion **45** (2003) S12A A17
[16] R.A. Pitts et al., submitted to Nucl. Mater. Energy (2016) - presented at PSI conference Rom
[17] M. Rieth et al., J. Nucl. Mater. **432** (2013) 482
[18] K. Piip et al., J. Nucl. Mater. **463** (2015) 919
[19] H. Reimerdes et al., 42nd EPS Plasma Physics, Lisbon, Portugal, ECA **39E** (2015) P4.117
[20] M. Wirtz et al., submitted to Nucl. Mater. Energy (2016) - presented at PSI conference Rom
[21] M. Wirtz et al., Nucl. Fus. **55** (2015) 123017
[22] P. Tolias et al., Plasma Phys. Control. Fusion **58** (2016) 025009
[23] S. Brezinsek et al., Nucl. Fus. **53** (2013) 083023
[24] A. Kirschner et al., this conference
[25] D. Tskhakaya et al., J. Nucl. Mater. **438** (2013) S522
[26] D. Moulton et al., Plasma Phys. Control. Fusion **55** (2013) 085003
[27] K. Dobes et al., Nucl. Instr. Meth. Phys. Research B **340** (2014) 34
[28] L. Gao et al., Nucl. Fus. **56** (2015) 016004
[29] A. Drenik et al., J. Nucl. Mater. **475** (2016) 237
[30] L. Laguardia et al., submitted to Nucl. Mater. Energy (2016) - presented at PSI conference Rom
[31] T. Dittmar et al., submitted to Nucl. Mater. Energy (2016) - presented at PSI conference Rom
[32] A. de Castro et al., J. Nucl. Mater. **463** (2015) 676
[33] J. Jepu et al., J. Nucl. Mater. **463** (2015) 983
[34] C.P. Lungu et al., private communication
[35] R. Mateus et al., - presented at the PFMC 2015 conference in Aix-en-Provence
[36] M. Pribula et al., Phys. Scr. **T167** (2016) 01404
[37] F. Colau et al., submitted to Nucl. Mater. Energy (2016) - presented at PSI conference Rom
[38] J. Xi et al., submitted to Nucl. Mater. Energy (2016) - presented at PSI conference Rom
[39] R. Bisson et al., this conference
[40] K. Schmid et al., Phys. Scr. **T167** (2016) 014025
[41] D. Kato et al., Nucl. Fus. **55** (2015) 083019
[42] S. Markelj et al., submitted to Nucl. Mater. Energy (2016) - presented at PSI conference Rom
[43] K. Sugiyama et al., J. Nucl. Mater. **463** (2015) 272
[44] P. Ström et al., Nucl. Instr. Meth. Phys. Research B **371** (2016) 355
[45] U. von Toussaint et al., Phys. Scr. **T167** (2016) 014023
[46] F.L. Tabares et al., submitted to Nucl. Mater. Energy (2016) - presented at PSI conference Rom
[47] E. Oyarzabal et al., J. Nucl. Mater. **463** (2015) 1173
[48] T. Morgan et al., submitted to Nucl. Mater. Energy (2016) - presented at PSI conference Rom
[49] A. Li-Puma et al., Fus. Eng. Des. **88** (2013) 1836-1843